Longwave plasmonics on doped silicon and silicides

Richard Soref, Robert E. Peale, and Walter Buchwald

Sensors Directorate, Air Force Research Laboratory, AFRL/RYHC, Hanscom Air Force Base, MA 01731-2909
Corresponding author: Richard.Soref@hanscom.af.mil

Abstract: The realization of plasmo-electronic integrated circuits in a silicon chip will be enabled by two new plasmonic materials that are proposed and modeled in this article. The first is ion-implanted Si (n-type or p-type) at the surface of an intrinsic Si chip. The second is a thin-layer silicide such as Pd_2Si, NiSi, $PtSi_2$ WSi_2 or $CoSi_2$ formed at the Si chip surface. For doping concentrations of 10^{20} cm^{-3} and 10^{21} cm^{-3}, our dispersion calculations show that bound surface plasmon polaritons will propagate with low loss on stripe-shaped plasmonic waveguides over the 10 to 55 μm and 2.8 to 15 μm wavelength ranges, respectively. For Pd_2Si/Si plasmonic waveguides, the wavelength range of 0.5 to 7.5 μm is useful and here the propagation lengths are 1 to 2300 μm. For both doped and silicided guides, the SPP mode field extends much more into the air above the stripe than it does into the conductive stripe material.

© 2008 Optical Society of America

OCIS codes: (240.6680) Surface plasmons; (250.5403) Plasmonics; (310.2790) Guided waves; (160.3918) Metamaterials; (160.3130) Integrated optics materials.

References and links

1. M. V. Bashevoy, F. Jonsson, A. V. Krasavin, and N. I. Zheludev, Y. Chen, M. I. Stockman, "Generation of traveling surface plasmon waves by free-electron impact," Nano Lett. **6**, 1113 (2006).
2. J. T. van Wijngaarden, E. Verhagen, A. Polman, C. E. Ross, H. J. Lezec, and H. A. Atwater, "Direct imaging of propagation and damping of near-resonance surface plasmon polaritons using cathodoluminescence spectroscopy," Appl. Phys. Lett. **88**, 221111 (2006).
3. S. Fan, R. A. Höpfel, E. Vass, and E. Gornik, "Thermal excitation of two dimensional plasma oscillations," Phys. Rev. Lett. **49,** 1667 (1982).
4. R. A. Soref, "The opto electronic integrated circuit," invited lead chapter in *Silicon Photonics—State of the Art*, G. T. Reed, eds., (John Wiley & Sons, Chichester, UK, to be published 2008).
5 R. A. Soref, "Towards silicon-based longwave integrated optoelectronics (LIO)," paper 6898-5 (invited) SPIE Photonics West, San Jose, CA, 21 January 2008 .
6. S. J. Bozhevolnyi and J. Jung, "Scaling for gap plasmon based waveguides", Optics Express, **16**, 2676-2684 (2008).
7. M. Amiotti, G. Guizzetti, F. Marabelli, A. Piaggi, V. N. Antonov, Vl. N. Antonov, O. Jepson, O. K. Anderson, A. Borghesi, F. Nava, V. V. Nemoshkalenko, R. Madar and A. Roualt, "Optical properties of Pd_2Si," Phys. Rev. **B 45**, 13285 (1992).
8. H. Raether, "Surface plasmon oscillations and their applications," in *Physics of Thin Films*, G. Hass, M. Francombe, and R. W. Hoffman, eds., (Academic Press, NY, 1977).
9. E. D. Palik, ed., *Handbook of Optical Constants of Solids*, (Academic Press, 1985) Vol. 1.

1. Introduction

Plasmonics refers to the technology in which surface plasmons are launched, transmitted, modulated, detected, etc, on sub-wavelength conducting structures formed on or within dielectrics or semiconductors. Plasmon optics is a subset of this technology in which the surface plasma polaritons (SPPs) are generated and detected optically. However, the SPPs can also be launched "electronically" by an electron beam [1,2] or by a MOSFET [3]. The latter case is most interesting because, as we described earlier [4], it will lead to silicon-based plasmo-electronic integrated circuits (PEICs) in which MOSFETs on the perimeter of a planar

#93263 - $15.00 USD Received 28 Feb 2008; revised 14 Apr 2008; accepted 16 Apr 2008; published 23 Apr 2008
(C) 2008 OSA

"plasmonic network" serve to launch and sense SPPs that are utilized by the plasmonic signal-processing circuits. This will be a CMOS-compatible, manufacturable IC.

A plasmon-optic circuit is also quite valuable because its sub-wavelength features facilitate the new technology of nano-photonics. In fact, plasmon optics (alongside photonic-crystal technology) is a key contributor to a "Moore's Law for photonics" which indicates that the on-chip packing density of integrated photonic components will increase year-by-year thanks to photonic research and development. In the long term, we can expect that plasmon optics will complement the plasmo-electronics discussed above; in other words, we shall eventually witness plasmo-optoelectronic integrated circuits (POEICs), a seamless integration of three techniques.

The prior art of plasmon optics utilized metal/dielectric and metal/semiconductor composites with their wavelengths generally in the visible or near infrared. In this paper, we focus upon non-metalized silicon substrates. We propose and analyze two new plasmonic materials that are probably more compatible with optoelectronics than are silver or gold films. These materials are highly doped-silicon embedded in undoped silicon, and a silicide film (e.g. $PtSi_2$, NiSi, Pd_2Si, WSi_2, $CoSi_2$) created in the undoped silicon surface. Both materials are "naturals" for fabrication in a silicon CMOS foundry. The doped-Si and silicided-Si SPP circuits interface seamlessly with their FET partners. Patterned doping can be accomplished in a well-known standard way by "shallow" implantation of ions into Si, or by in-diffusion through a mask. Formation of silicides on Si by metal deposition, thermal reaction, and conversion-to-silicide is also well known in the industry.

The wavelengths for prior-art metal-delectric-metal SPP based waveguides are in the near infrared, but as we shall show in this article, the doped-Si and silicided-Si offer low-loss performance not in the NIR, but rather in the mid-wave, longwave and very longwave infrared. Our generic term "longwave" is shorthand for these three spectral regions [5]. The longwave SPP circuit or "network" will perform signal processing functions on the Si chip. If the footprint of the network is sufficiently small, if the processing is fast, and if the power consumption is quite low, then *the wavelength and frequency of the plasmons are immaterial*. We anticipate that the longwave SPP circuit will meet the size-speed-power requirements, making the longwaves "viable".

The organization of this paper is as follows: we first propose striped and slotted structures for channel waveguides, then we compile the relevant surface plasmon properties calculated from the complex permittivity. These properties include the dispersion curves with their bound and free modes, the propagation losses within feasible longwave regions, and the mode profiles with estimated penetration depths into the air and the conductive medium.

2. Waveguide structures

Two structures that are beneficial for plasmonic circuits are the simple stripe and the parallel-stripe "slotted" plasmonic waveguides [6]. These are illustrated in Fig. 1 for the cases of doped Si and silicide-on-Si. The vertically stacked double-plasmonic waveguide (not shown

#93263 - $15.00 USD Received 28 Feb 2008; revised 14 Apr 2008; accepted 16 Apr 2008; published 23 Apr 2008
(C) 2008 OSA

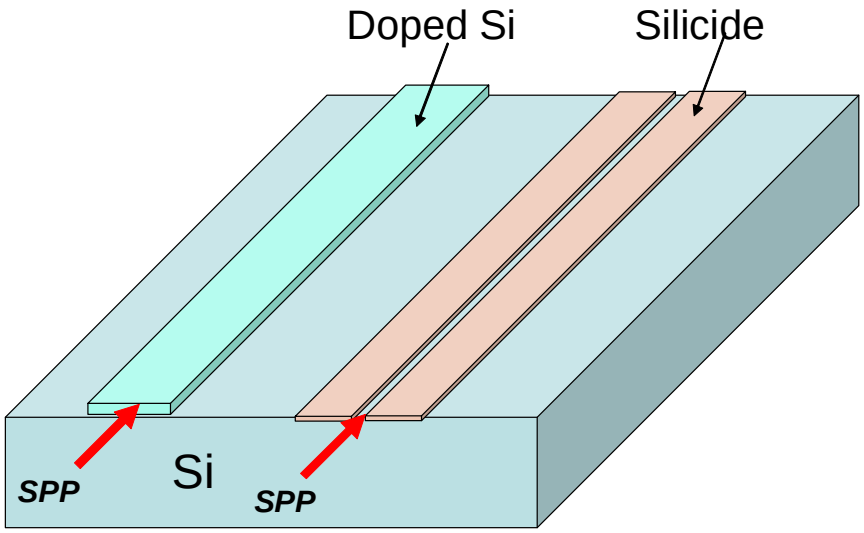

Fig. 1. Silicon CMOS-compatible plasmonic channel waveguides utilizing ion-implanted Si and silicided Si.

here) will also work quite well. It consists of two plane-parallel conductive stripes (doped or silicided) that are separated by a dielectric layer. We begin our analysis of waveguiding by examining the permittivity data for p-type Si, n-type Si, Pd_2Si and a prior-art reference material (gold).

3. Complex permittivity data

The SPP properties that can be calculated from the permittivity include the complex wavevector, the propagation length $\mathcal{L}$ for the SPP intensity along the surface, the SPP spatial confinement as determined by the distance L_{air} that the field extends into air above the waveguide surface and by the field penetration L_{cond} into the doped or silicided conductor. As a concrete example of a silicide where at least some empirical information exists [7] for the complex permittivity $\varepsilon(\omega)$ we choose Pd_2Si. Doped Si supposes P or B dopants at levels of 10^{20} and 10^{21} cm^{-3}. Empirical $\varepsilon(\omega)$ data for either materials system is presently incomplete in the longwave regime, so we use instead theoretical extrapolation based on the Drude model.

To determine the longwave permittivity from the available near-IR measurements, the Drude model gives

$$\varepsilon(\omega) = \varepsilon'(\omega) + \imath\, \varepsilon''(\omega) = \varepsilon_\infty - \omega_p^2/[\omega^2\,(1+\imath\,/\omega\tau)], \qquad (1)$$

where ε_∞ is the permittivity for $\omega >> \omega_p$, the plasma frequency is ω_p, and τ is the electron relaxation time. For doped Si, τ is determined from the empirical drift mobility $\mu = e\tau/m^*$, where m^* is the orientationally averaged electron effective mass $m^* = 0.272\ m_0$, $\varepsilon_\infty = 11.7$, and $\omega_p^2 = Ne^2/\varepsilon_0 m^*$, with N the electron concentration per cm^3. The mobility at the two concentrations considered here is ~50 cm^2/V-s. For Pd_2Si, and an orientationally averaged plasma frequency of 3.1 eV, a relaxation time of $1/\tau = 0.03$ eV [7], and $\varepsilon_\infty = 1$ were used. SPPs are supported at frequencies wherever ε' is negative. For Pd_2Si, unlike gold, the probability of SPP generation by electron beams, given by $\mathrm{Im}[-1/(1-\varepsilon)]$, extends deep into the infrared [8]. Longwave SPPs are also generated efficiently in highly doped Si. Little is known about the infrared permittivity of the novel Si-compatible narrow-gap single-crystal

#93263 - $15.00 USD Received 28 Feb 2008; revised 14 Apr 2008; accepted 16 Apr 2008; published 23 Apr 2008
(C) 2008 OSA

GeSn films, but their intrinsic conductivity approaches 10^{20} cm^{-3} with Drude model parameters expected to be comparable to Ge. Thus this alloy also has SPP promise.

Figures 2(a) and 2(b) present the real and imaginary parts of the complex permittivity of our four materials. The Fig. 2(a) plot of Re[ε(ω)], or ε′(ω) in Eq. (1), shows that SPPs are supported on Si for frequencies ω corresponding to optical wavelengths longer than 7 μm for 10^{20} cm^{-3} doping and longer than 2 μm for 10^{21} cm^{-3} doping. For Pd_2Si and gold, the high energy curves are empirical values [7, 9] and the low energy sections are our calculated Drude-model values. For the silicide, SPPs can be sustained throughout the visible and infrared. Figure 2(b) presents Im[ε(ω)], or ε″(ω) in Eq. (1). For the silicide, ε″ is significantly larger than for gold in the visible and NIR, suggesting higher loss, but the small Pd_2Si damping parameter $\gamma = 1/\tau$ of only 0.03 eV [7] results in a calculated Drude curve that is significantly lower than for gold in the mid- and far-infrared. The large discontinuity between empirical- and Drude-based permittivity ε″ values emphasizes the lack of experimental infrared data for the silicide.

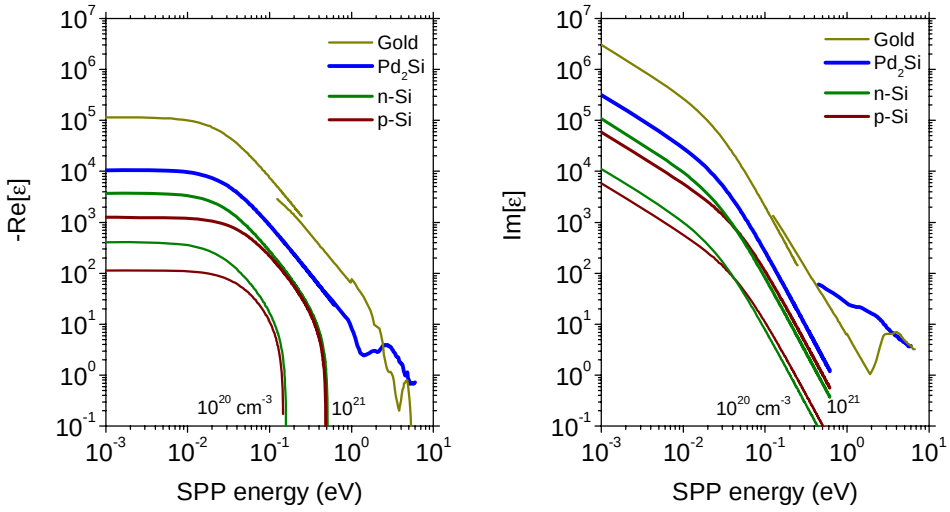

Fig. 2. Permittivities –ε′(ω) and ε″(ω)of doped-Si and Pd_2Si compared with those of gold.

4. Bound SPPs for plasmonic waveguides

We next calculate the ω-*k* dispersion curves for our materials; the dependence of the SPP energy as a function of the real SPP wave vector *k*′. The complex SPP wavevector for the vacuum-"metal" interface is determined from the complex permittivity ε of the metal, according to

$$k = (\omega/c)\sqrt{[\varepsilon(\omega)/(1+\varepsilon(\omega))]} \qquad (2)$$

where ω is the angular frequency, and c is the speed of light. The results are presented in Fig. 3(a) showing the SPP dispersion curve ω *vs* the real wavevector *k*′ for doped silicon. The curves for both impurity concentrations fall below the light line ω = c *k* at low wavevector, but rather than saturating at $\omega_p/\sqrt{2}$ as for ideal free-electron metals, there is an inflection point where the curve jumps to the upper polariton branch. The above-lightline branch refers to radiative SPPs which are not really useful on our chip, whereas the below-lightline branches describe the bound SPPs desired in our waveguided circuit.

Judging from Fig. 3(a), the lower limit of the useful wavelength range ought to be where the SPP branch crosses over the lightline. However, the actual lower wavelength limits will be

#93263 - $15.00 USD Received 28 Feb 2008; revised 14 Apr 2008; accepted 16 Apr 2008; published 23 Apr 2008
(C) 2008 OSA

determined from a different criterion based upon the propagation lengths discussed below. The usual distinct polariton branches appear if τ is artificially increased by about two orders of magnitude such that $\omega\tau$ becomes >> 1. Unless that condition is fulfilled, the imaginary part of the permittivity is significant [Eq. (1)], suggesting high loss. For the doping concentrations considered, $\omega\tau$ is only of order unity in the infrared, therefore the Fig. 2(a) S-shaped SPP dispersion is a feature of a fairly small relaxation time (fairly large dissipation). Decreasing ε_∞ similarly makes the curve more polariton-like.

Figure 3(b) compares the dispersion curves for Pd_2Si and gold using empirical permittivity data [7, 9]. A slight S-shaped kink in the SPP dispersion curve exists for gold at ~500 nm optical wavelength, similar to the infrared situation for doped semiconductors, because of d-state absorption loss in the visible. The dispersion curve for Pd_2Si generally hugs the light line throughout the spectrum, although this curve is actually "microscopically below" the light line, allowing bound SPP propagation over a wide energy range. Experimentally, we have obtained evidence of SPPs excited on Pd_2Si at long waves using a grating coupler and a CO_2 laser, results that will be published elsewhere

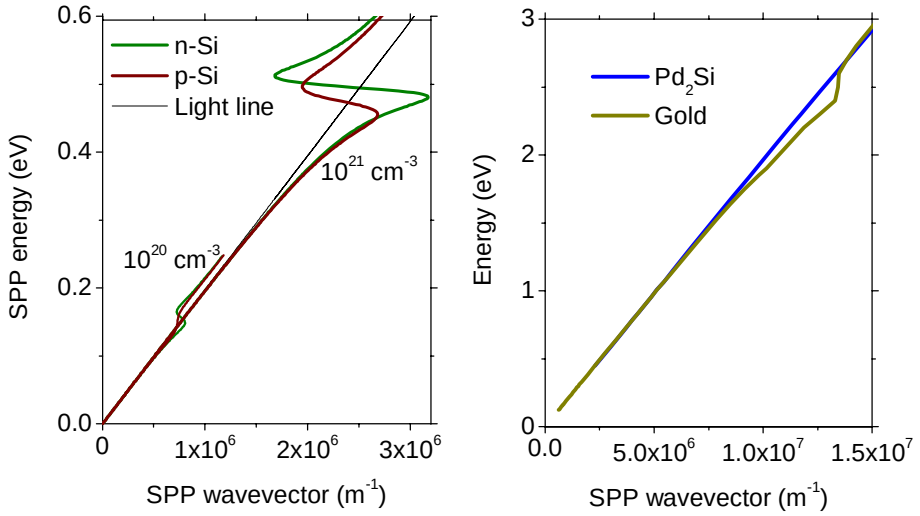

Fig. 3. (left) SPP dispersion curves for doped silicon; (right) SPP dispersion curves for gold and Pd_2Si.

5. Mode propagation loss

The characteristic propagation length $\mathcal{L}$ for SPP intensity is $\mathcal{L}^{-1} = 2\,\mathrm{Im}[k]$ and we turn to Eq. (2) along with Fig. 2 to determine $\mathcal{L}$ as a function of SPP energy $h\nu$. Figure 4 presents and compares our predicted SPP propagation lengths for the four plasmonic materials. The SPP wavelengths $2\pi/k'$ are nearly the same as the optical wavelengths λ at the two SPP frequencies since the dispersion curve is close to the light line. At the SPP short-wavelength limits of 8 μm and 2.5 μm, Fig. 4 reveals that $\mathcal{L}$ is comparable to λ, a critically damped situation where one can hardly speak of a group velocity or the propagation of information. Therefore we shall demand that $\mathcal{L}$ is twice λ to make the lower limit practical. Doing that, we then find from Fig. 4 that the useful minimum wavelengths are 3 μm for 10^{21} cm^{-3} and 9 μm for 10^{20} cm^{-3}.

For the silicide, propagation lengths are always less than those for gold. Nevertheless they are still very long in the long-wave IR and THz. Applying the $\mathcal{L} = 2\lambda_{low}$ criterion shows that

#93263 - $15.00 USD Received 28 Feb 2008; revised 14 Apr 2008; accepted 16 Apr 2008; published 23 Apr 2008
(C) 2008 OSA

silicide is suitable for propagating information well into the visible. Also, $\mathcal{L}$ exceeds λ by factors of order 1000 in the longwave infrared, showing that SPP's in silicide are underdamped in that region. Our $\mathcal{L}$ calculations with $\mathcal{L} = 2\lambda_{low}$ predict minimum useful free-space wavelengths of 0.5, 0.5, 2.8 and 10 μm, respectively, for gold, Pd_2Si, doped Si at 10^{21}, and doped Si at 10^{20}. The calculated ~1 cm propagation length for gold at 0.1 eV has been experimentally verified by us, as will be described elsewhere.

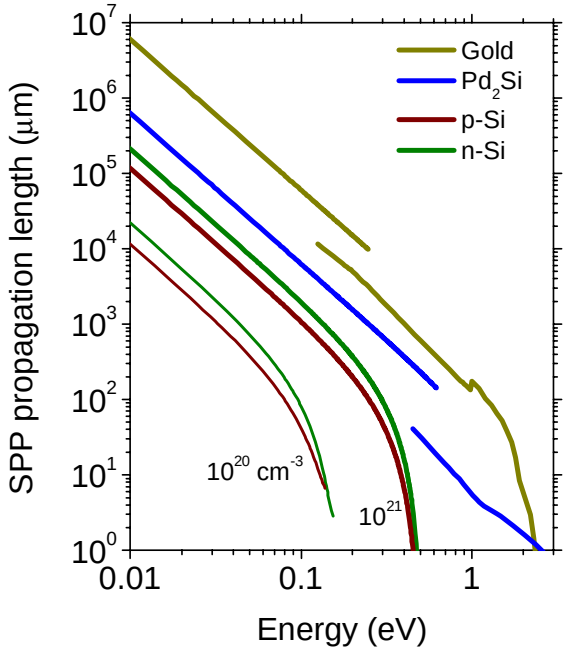

Fig. 4. SPP propagation length on doped Si, Pd_2Si, and gold.

6. Mode profile

Assuming an air cladding above the stripe-shaped plasmonic silicon waveguide, we next ask how the SPP field fringes out into the air above and into the conductive material below the Si surface. The penetration length of the Z-propagating wave is defined as the lateral dimension X at which the field strength decreases to 1/e of its initial value. The SPP fields extend above the surface by an amount L_{air} and penetrate into the conductor by an amount L_{cond} with $L_{air} = (c/\omega)/\mathrm{Re}[\sqrt{(-1/(1+\varepsilon))}]$ and $L_{cond} = (c/\omega)/\mathrm{Re}[\sqrt{(-\varepsilon^2/(1+\varepsilon))}]$ where ε is given in Fig. 2.

For SPPs propagating in the Z direction, Fig. 5 presents results of our X-penetration calculations for fields into the media on either side of the surface. The Fig. 5 inset shows these penetrations schematically. Generally, the mode fringing into air is much larger than the conductor penetration. The penetration depth into the doped silicon is < 0.6 μm. Uniform doping of the silicon surface to depths of 1 μm is readily achieved by diffusion or ion-implantation. Thus, surface-doped silicon can behave as bulk material as far as SPPs are concerned. This is a very important observation for making SPP waveguides by patterned diffusion or implantation on future PEIC devices. For silicide, the mode penetration into air grows very large at the longest wavelengths. By contrast, the mode penetration into Pd_2Si is < 70 nm at all wavelengths, which means that a very thin silicide layer, such as 100 nm, will suffice as an SPP host, and that is advantageous for devices.

#93263 - $15.00 USD Received 28 Feb 2008; revised 14 Apr 2008; accepted 16 Apr 2008; published 23 Apr 2008
(C) 2008 OSA

We suppose that the longwave limit for usefulness in a PEIC is when the confinement amounts to ~ 3 wavelengths, i.e., we impose the condition that $L_{air} = 3\ \lambda_{high}$. According to this, the usefulness of gold ends at $\lambda \sim 3$ μm. For Pd_2Si, it occurs at 7.5 μm, while for doped Si, it is 55 μm and 15 μm, respectively for 10^{20} cm^{-3} and 10^{21} cm^{-3}. Confinement can be increased by using a transparent polymer overlay instead of air. That would extend the silicide limit well beyond 7.5 μm. The specific mode penetration results for doped Si and silicided Si are summarized in Table 1 together with our predictions of the useable wavelength range and the mode propagation length

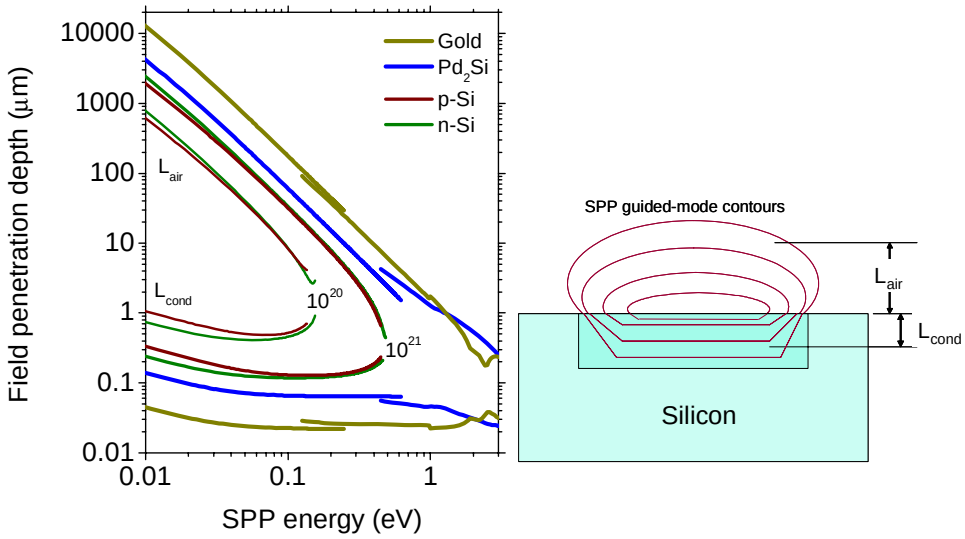

Fig. 5. SPP field penetration lengths into the media on either side of the surface. (0.1 eV corresponds tothe 12.4 micron optical wavelength.)

Table 1. Predicted performance of Si-based plasmonic channel waveguides

Material	useful λ range (μm)	ℓ (μm)	L_{air} (μm)	L_{cond} (μm)
Gold	0.5 - 3.0	1 - 1000	0.25 - 9.0	0.03 - 0.025
Pd_2Si	0.5 - 7.5	1 - 2300	0.25 - 22.5	0.024 - 0.064
10^{21} cm^{-3} doped Si	2.8 - 15	5.6 - 3000	0.7 - 45	0.23 - 0.13
10^{20} cm^{-3} doped Si	10 - 55	20 - 4300	4.9 - 165	0.53 - 0.50

7. Conclusion

We have predicted the performance of silicon-based plasmonic waveguides for two new SPP materials that can be fabricated readily in a CMOS foundry using standard processing techniques such as salicidation and shallow implantation or diffusion of B and P ions into

#93263 - $15.00 USD Received 28 Feb 2008; revised 14 Apr 2008; accepted 16 Apr 2008; published 23 Apr 2008
(C) 2008 OSA

intrinsic crystal silicon. For doped Si, we estimate that the practical SPP wavelength ranges are 10 to 55 μm and 2.8 to 15 μm for donor/acceptor concentrations of 10^{20} cm^{-3} and 10^{21} cm^{-3}, respectively. At a given wavelength, the SPP propagation lengths $\mathcal{L}$ are at least one order-of-magnitude longer at the higher doping density. The Pd_2Si offers a low-loss waveguide solution over a wavelength range that is intermediate between the noble-metal range and the doped silicon range. Our analysis shows that bound SPP fields penetrate more into the air than the into the conductive stripe.

Acknowledgment:

The authors wish to thank AFOSR/NE (Dr. Gernot Pomrenke, Program Manager) for ongoing support of this in-house research. Robert Peale is on sabbatical at AFRL from the University of Central Florida, Department of Physics.

#93263 - $15.00 USD Received 28 Feb 2008; revised 14 Apr 2008; accepted 16 Apr 2008; published 23 Apr 2008
(C) 2008 OSA